

COMMUNICATION

# Effective encapsulation of C<sub>60</sub> by metal-organic frameworks with polyamide macrocyclic linkers

Adrian Saura-Sanmartin,<sup>[a]</sup> Alberto Martinez-Cuezva,<sup>[a]</sup> Marta Marin-Luna,<sup>[a]</sup> Delia Bautista,<sup>[b]</sup> and Jose Berna<sup>[a],\*</sup>

[a] A. Saura-Sanmartin, Dr. A. Martinez-Cuezva, Dr. M. Marín-Luna, Dr. J. Berna\*  
Departamento de Química Orgánica, Facultad de Química, Regional Campus of International Excellence "Campus Mare Nostrum", Universidad de Murcia, E-30100 Murcia (Spain).  
E-mail: ppberna@um.es

[b] Dr. D. Bautista  
Sección Universitaria de Instrumentación Científica (SUIC), Área Científica y Técnica de Investigación (ACTI), Universidad de Murcia, E-30100 Murcia (Spain)

Supporting information for this article is given via a link at the end of the document.

**Abstract:** A flexible benzylic amide macrocycle, functionalized with two carboxylic acid groups, was employed as the organic ligand for the preparation of robust copper(II)- and zinc(II)-based metal-organic frameworks. These polymers crystallized in the C2/m space group of the monoclinic crystal system, creating non-interpenetrated channels in one direction with an extraordinary solvent-accessible volume of 46%. Unlike metal-organic rotaxane frameworks having benzylic amide macrocycles as linkers, the absence of the thread in these novel reticular materials causes a decrease of dimensionality and an improvement of pore size and dynamic guest adaptability. We studied the incorporation of fullerene C<sub>60</sub> inside the adjustable pocket generated between two macrocycles connected to the same dinuclear clusters, occupying a remarkable 98% of the cavities inside the network. The use of these materials as hosts for the selective recognition of different fullerenes was evaluated, mainly encapsulating the smaller size fullerene derivative in several mixtures of C<sub>60</sub> and C<sub>70</sub>.

Over the last decades, the design of innovative porous materials for relevant applications such as gas storage, analyte separation, or catalysis is a research field of substantial activity.<sup>1</sup> Metal-organic frameworks (MOFs) are a fascinating family of crystalline porous materials constituted by metal clusters and organic ligands.<sup>2</sup> Boosting complexity of MOFs is one of the key strategies to prepare materials with upgraded functionalities. The number of possible combinations of the metal sources<sup>3</sup> with the organic ligands, plus their particular geometries, is nearly unlimited,<sup>4</sup> leading to a variety of materials with different morphologies, pore size distributions and functionalities.<sup>5</sup>

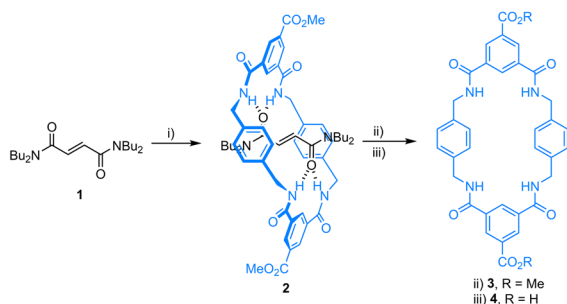
The most common organic ligands used in the preparation of MOFs are small and rigid multidentate molecules bearing carboxylic acid linkers. Under solvothermal conditions, the deprotonation of the acidic protons and the subsequent coordination of the carboxylate groups to a metal core easily happened, forming robust and stable architectures.<sup>6</sup> In contrast, the use of large and flexible ligands is less established, likely due to a lower thermal stability of the networks and to a less reproducible assembly.<sup>7</sup> In spite of these shortcomings, large macrocycles,<sup>8</sup> including crown ethers,<sup>9</sup> ethynylene-derived

macrocycles,<sup>10</sup> cyclic polyamines,<sup>11</sup> cyclodextrins,<sup>12</sup> calixarenes,<sup>13</sup> cucurbiturils,<sup>14</sup> or pillarenes,<sup>15</sup> between others, have been successfully incorporated in the widespread ligand tool-box. One advantage in the use of these ligands is the presence of large and well-ordered recognition cavities, highly valuable for the establishment of noncovalent interactions with suitable guests.<sup>16</sup>

The wide range of structural motifs found in MOFs makes them excellent candidates for host-guest chemistry, being used as selective receptors for small molecules including gases, hydrocarbons and alcohols among others.<sup>17</sup> The recognition of relatively large molecules is still underexplored in this field due to the difficulty of the bulky guests to diffuse into the network pores. For instance, the selective recognition of fullerenes<sup>18</sup> has been widely studied in solution by using supramolecular cages and nanocapsules,<sup>19</sup> molecular tweezers,<sup>20</sup> macrocycles<sup>21</sup> or small polymers<sup>22</sup> as receptors. However, only a scarce number of examples in the use of MOFs for this particular purpose have been disclosed.<sup>23</sup>

Herein, we describe the building of copper(II)- and zinc (II)-organic frameworks that incorporate a benzylic amide macrocycle bearing two carboxylic acid linkers as a ditopic ligand. We have previously reported the preparation of metal-organic frameworks by using similar but interlocked macrocycles in the form of [2]rotaxanes.<sup>24</sup> Thus, the results of the present work will allow to compare how the absence or presence of the mechanical bond affects the molecular arrangement of nearly identical constituents (macrocycle vs rotaxane) in the crystalline network. The novel metal-organic structures were elucidated by X-ray diffraction, showing 1D networks that form channels along the *c* axis. The void between two concave macrocycles offers a complementary volume for the accommodation of fullerene derivatives, allowing the application of these materials as selective hosts of C<sub>60</sub> in mixtures with other fullerenes.

En route to metal-organic frameworks having large pores we decided to employ a benzylic amide-based macrocycle as organic ligand. First, we synthesized the polyamide macrocycle **4**, with a carboxylic acid group at each isophthalamide unit (Scheme 1). Benzylic amide macrocycles of this type are usually obtained in



**Scheme 1.** Synthesis of the benzylic amide macrocycle **4**. *Reaction conditions:* i) *p*-xylylenediamine, methyl 3,5-bis(chlorocarbonyl)benzoate, Et<sub>3</sub>N, CHCl<sub>3</sub>, 25 °C, 4 h, 34%; ii) DMSO, 100 °C, 12 h, 99%; iii) LiOH·H<sub>2</sub>O, THF, reflux, 48 h, 99%.

low yields through a (2+2) condensation of *p*-xylylenediamine and an aroyl dichloride, together with the corresponding catenanes (main reaction products) and a complex mixture of oligomers of different size.<sup>25</sup> Moreover, these tetralactams are very insoluble in halogenated solvents (less than 1 mg/L in CHCl<sub>3</sub>),<sup>25c</sup> making their purification highly problematic. To avoid these issues, we followed an amenable three-step synthetic protocol for the obtention of **4** (Scheme 1). Initially, the five-component coupling reaction<sup>26</sup> between a tetraalkylfumaramide thread **1**, *p*-xylylenediamine and methyl 3,5-bis(chlorocarbonyl)benzoate led to the kinetically stable [2]pseudorotaxane **2** in 34% yield (see section 2 of the Supporting Information for the complete synthetic procedure).<sup>27</sup> The thermal treatment of rotaxane **2** in a highly polar solvent, such as DMSO, efficiently promoted the dethreading process<sup>28</sup> thus affording the macrocycle **3** in a practically quantitative manner. Finally, the saponification reaction of the ester groups of **3** in basic media gave the macrocycle **4** in 99% yield, having two carboxylic acid groups at both C5 positions of the isophthalamide units.<sup>29</sup>

The metal-organic frameworks UMUMOFs **5** were readily prepared by following a solvothermal protocol (Figure 1, see section 3 of the Supporting Information for further details).<sup>30</sup> The Cu(II)-based polymer, named UMUMOF **5a**, was obtained by reaction of Cu(NO<sub>3</sub>)<sub>2</sub>·H<sub>2</sub>O with the macrocyclic ligand **4** in a 3:3:2 DMF/EtOH/H<sub>2</sub>O mixture. After heating at 80 °C in a temperature-controlled oven for 48 h, followed by slow cooling to room temperature at a rate of 0.05 °C·min<sup>-1</sup> (Figure S1), light blue discorrectangle-shaped crystals were collected in 72% yield (Figure 1c and Image S1). The polymeric structure was successfully elucidated by single-crystal X-ray diffraction<sup>31</sup> revealing that UMUMOF **5a** crystallizes in the C2/m space group of the monoclinic crystal system with an overall formula of [Cu<sub>2</sub>(**4**)<sub>2</sub>(H<sub>2</sub>O)<sub>2</sub>]<sub>n</sub>·*n*H<sub>2</sub>O. The crystalline topology revealed 1D-periodic linear polymers<sup>32</sup> having bent macrocyclic ligands connected through the carboxylate groups to the dimeric Cu(II) paddlewheel clusters (Figure 1a,b). Each cluster is coordinated to four different macrocycles having two water molecules at its axial positions. The angle between two macrocyclic units linked to the same cluster is 77.5°. The dimension of the channel created between two copper clusters and two macrocycles is defined by the distance between the Cu(II) paddlewheels (19.47 Å) and the distance of the centroids of the *p*-xylylene rings of each macrocycle (10.96 Å). Interestingly, we have previously reported the building of 2D-periodic Cu-based metal-organic frameworks by using rotaxane ligands bearing similar tetralactam

macrocycles.<sup>24</sup> In those materials the presence of an interlocked thread inside the macrocyclic cavity precluded the formation of 1D polymers such as in **5a**. The absence of the thread in the novel UMUMOF **5a** is shown to cause an increase in flexibility and a larger pore size, probably due to the larger conformational space of the non-interlocked macrocyclic ligand and the lesser steric demand in comparison to that of a rotaxane<sup>24,33</sup> having the same macrocycle.

A similar synthetic procedure was followed for the preparation of the Zn(II)-based framework **5b**, by using Zn(OAc)<sub>2</sub>·2H<sub>2</sub>O as the metal source and DMF as the sole solvent, obtaining colourless prismatic crystals (Image S2) in 62% yield (see Supporting Information for further experimental details). UMUMOF **5b** presents an X-ray structure<sup>31</sup> similar to that of **5a**, consisting of a Zn(II) paddlewheel (two zinc atoms) coordinated to four different macrocycles through their carboxylate groups. Similarly, two water molecules are placed at the axial positions of the dinuclear metallic cluster (Figure S12). The angle between the two macrocycles is 77.7°. The void generated by two macrocycles and two metal clusters is slightly larger than that of **5a**, with dimensions of 19.50 x 11.21 Å.

The macrocycles in UMUMOFs **5** are organized in stacked corrugated layers along the *b*-axis (Figure 2 for **5a**), stabilized by hydrogen bonding interactions between the CO moieties of a group of interconnected macrocycles and the NH groups of the neighbour (Figures S10-11 and S13-14). Stabilizing π-π stacking interactions between the aromatic ring of the *p*-xylylene motif of a strand of macrocycles with the bordering one along the *c*-axis are also established. In the case of **5a** (Figure 2), this arrangement forms well-defined and ordered channels along the *c*-axis, with a total cell volume of 4869 Å<sup>3</sup> and a calculated solvent-accessible volume of 2246 Å<sup>3</sup> (46% of the total volume).<sup>34,35</sup>

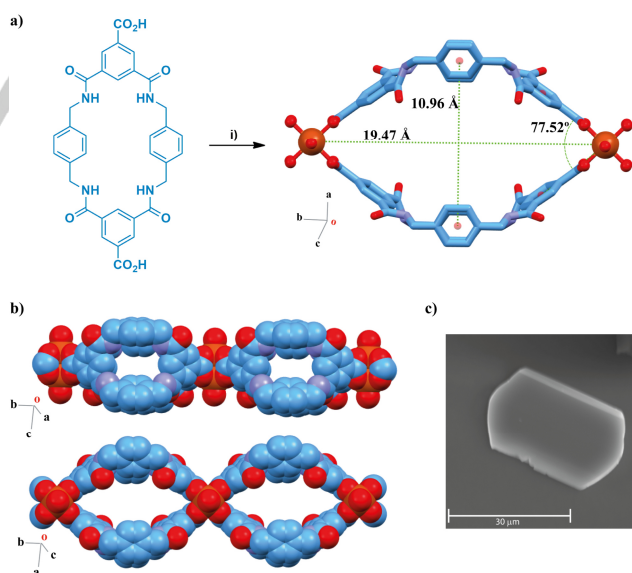


**Figure 1.** Preparation of UMUMOF **5a**. a) capped-sticks representation of the unit cell of **5a**; b) spacefill representation of the pocket of two connected macrocycles of UMUMOF **5a** along the *a* axis and the *c* axis; c) scanning electron microscopy image of one crystal of **5a**; *Reaction conditions:* i) Cu(NO<sub>3</sub>)<sub>2</sub>·H<sub>2</sub>O, HNO<sub>3</sub> (cat), DMF:EtOH:H<sub>2</sub>O (3:3:2), 80 °C.

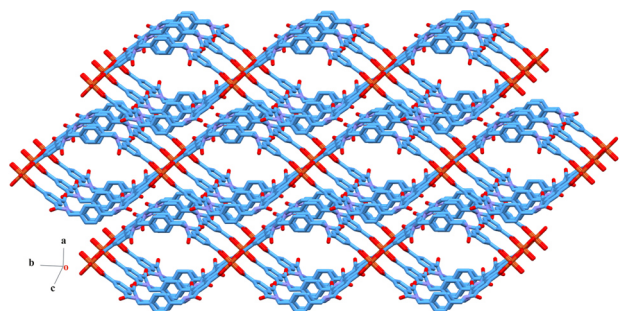


**Figure 2.** Linked frameworks of **5a** forming channels along the c-axis (hydrogen atoms are omitted for clarity).

Furthermore, UMUMOFs **5** were fully characterized by means of elemental analysis, infrared spectroscopy, thermogravimetric analysis, and powder X-ray diffraction analysis. The IR analyses (Figures S4-6) of **5a** showed the asymmetric and symmetric stretching vibrations between the carboxylate functionalities and the copper ions, with the respective values of 1643.28 and 1305.42  $\text{cm}^{-1}$ .<sup>36</sup> In the case of the zinc analogue **5b**, the corresponding carboxylate-zinc bands were also observed (asymmetric stretching 1667.95  $\text{cm}^{-1}$  and symmetric stretching 1302.79  $\text{cm}^{-1}$ ).<sup>36</sup> The powder diffraction patterns confirmed that the as-synthesized structures are crystalline, maintaining their well-ordered network after thermal activation (Figures S7-8). The stabilities of **5a,b** were examined by TG analyses under nitrogen stream between 20-1000 °C at a heating rate of 5 °C/min (Figure S16) pleasantly showing a robust thermal stability. For both materials, there are small weight losses under 220 °C related to residual solvents in the interstices of the polymeric network, as well as solvents hydrogen-bonded to the NH groups of the macrocycle. Above 300 °C, main weight losses were observed due to the collapse of the frameworks.

The boat conformation of the benzylic amide macrocycles<sup>37</sup> in these materials generates concave curvatures towards the inner of the channels, building well-ordered cavities with relatively large dimensions. The magnitude of these voids made us to consider the incorporation of fullerene derivatives inside the polymeric array. The reported van der Waals diameter of fullerene  $\text{C}_{60}$  (ca 10.4 Å)<sup>38</sup> is slightly smaller than that of the pocket (10.96 Å for **5a**; 11.21 Å for **5b**), and thus it could reasonably fit inside the channels. Furthermore, eight aromatic rings facing the interior of the cavity could probably establish  $\pi$ - $\pi$  stacking interactions with the fullerene derivatives.<sup>39</sup> With this aim, we soaked crystals of **5a,b** in a  $\text{C}_{60}$  saturated toluene solution<sup>40</sup> at room temperature for seven days. Disappointingly, no incorporation of  $\text{C}_{60}$  inside the polymeric materials was detected under these conditions. We repeated the loading process at 60 °C observing that the crystals gradually turned black over time. The dark crystals were filtered, washed exhaustively with toluene until fullerene was not detected in the washings by TLC,<sup>41</sup> and dried under vacuum for several hours (Image S3). Elemental analyses revealed that the incorporation of fullerene inside the frameworks certainly happened under these conditions, measuring a significant increase in the carbon percentage of the loaded materials **C<sub>60</sub>@5** if compared with the empty MOFs: 56.25% for **5a** versus 68.75% for **C<sub>60</sub>@5a**, and 57.96% for **5b** versus 64.25% for **C<sub>60</sub>@5b**. Thermogravimetric analyses also confirmed the successful fullerene encapsulation by using UMUMOFs **5** (Figure S16).

Carbon dioxide adsorption experiments<sup>42</sup> also supported this conclusion, showing a decrease in the adsorbed gas volume for the loaded materials **C<sub>60</sub>@5** compared to UMUMOFs **5** (Figure S28). Apparently, in the warm toluene solution at 60 °C a breathing of the MOF occurs, enlarging the pore dimensions of the material and, consequently, allowing the diffusion of the fullerene inside the cavities.<sup>43</sup>

Next, the reversible releasing of the fullerene from the metallic networks was investigated. We immersed the  $\text{C}_{60}$  loaded UMUMOFs **C<sub>60</sub>@5** in carbon disulfide (method A) or *o*-dichlorobenzene (method B), solvents with high affinity for fullerene derivatives (see section 7 of the Supporting Information for further details).<sup>44</sup> Method A allowed a quick and complete release of  $\text{C}_{60}$  from inside the frameworks but caused a partial collapse of the polymeric network. Method B was slower, although retaining the structural integrity of the coordination polymer as further proved by an XPRD analysis (Figure S29).<sup>45</sup> Using Beer-Lambert's law, we determined a loading of 33.6 wt% of  $\text{C}_{60}$  in **5a** and 14.4 wt% in the case of **5b**. These data revealed an impressive calculated occupation of 98% of the UMUMOF **5** cavities in **C<sub>60</sub>@5a** and of 42% in **C<sub>60</sub>@5b**. The higher occupation determined for **5a** could be attributed to the smaller dimensions of the pockets between macrocycles compared to **5b**, thus precluding the rapid diffusion of  $\text{C}_{60}$  from the material, once loaded, to the solution during the loading process. UMUMOF **5a** is one of the MOFs with the highest  $\text{C}_{60}$  loading efficiency reported so far.<sup>23</sup>

We next evaluated the ability of these systems as containers for the selective recognition of fullerene derivatives ( $\text{C}_{60}$  vs  $\text{C}_{70}$ ), having in mind the restricted pore dimensions and the difference in the van der Waals radii of the guests (10.4 Å for  $\text{C}_{60}$  and 10.9 Å for the shorter length in  $\text{C}_{70}$ ).<sup>38</sup> Table 1 summarizes the data obtained from the competitive loading experiments. As an initial point, we soaked crystals of **5a,b** in a solution of pure  $\text{C}_{70}$  in toluene at 60 °C for seven days, not detecting its incorporation into the coordination polymer (Table 1, entries 1-2). In contrast, when crystals of **5a,b** were loaded with solutions of different  $\text{C}_{60}:\text{C}_{70}$  ratios, we observed minor incorporation of  $\text{C}_{70}$ . Starting from a 75:25  $\text{C}_{60}:\text{C}_{70}$  mixture, UMUMOF **5a** preferentially encapsulated the smaller fullerene with a 96:4  $\text{C}_{60}:\text{C}_{70}$  ratio (Table 1, entry 3). Similarly, material **5b** also incorporated  $\text{C}_{60}$  as the main guest, although with slightly lower selectivity (91:9  $\text{C}_{60}:\text{C}_{70}$  ratio, Table 1, entry 4). When using a 50:50 mixture of  $\text{C}_{60}:\text{C}_{70}$ , the smaller  $\text{C}_{60}$  partner was again selectively incorporated inside the networks (Table 1, entries 5-6) in 88:12 ratio with UMUMOF **5a**, and in 81:19 ratio with UMUMOF **5b**. Finally, from a  $\text{C}_{70}$ -enriched mixture (20:80  $\text{C}_{60}:\text{C}_{70}$  ratio), the reversed 80:20  $\text{C}_{60}:\text{C}_{70}$  ratio was incorporated in both loaded materials (Table 1, entries 7-8). The lower selectivity generally shown by **5b** is reasonably attributed to its larger pore when compared to that of **5a**.

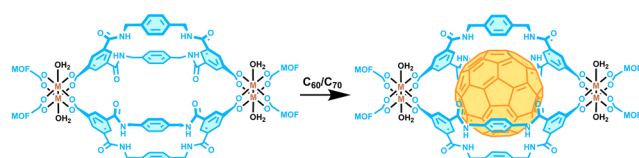
We were intrigued by the fact that in our hands UMUMOFs **5** were not able to incorporate pure  $\text{C}_{70}$  whereas, in sharp contrast, a minor amount of this fullerene was loaded into the network from  $\text{C}_{60}:\text{C}_{70}$  mixtures. In order to rationalize these results, we hypothesized that, after the initial incorporation of  $\text{C}_{60}$  inside the cavities of these MOFs, a slight distortion of the framework could occur, resulting in an expansion of its initial pore size. Under this scenario, the bulkier  $\text{C}_{70}$  could be then incorporated. To evaluate this idea, we performed the following experiment: we exhaustively released  $\text{C}_{60}$  from the loaded material **C<sub>60</sub>@5a** by treatment with



## COMMUNICATION

*o*-dichlorobenzene (method B) and then immersed the resulting porous material (presumably with already distorted pores<sup>44</sup>) in a

**Table 1.** C<sub>60</sub> and C<sub>70</sub> competitive loading experiments with UMUMOFs 5.



| entry | UMUMOF                   | C <sub>60</sub> :C <sub>70</sub> ratio | Incorporated C <sub>60</sub> :C <sub>70</sub> [a] |
|-------|--------------------------|--|---|
| 1     | <b>5a</b>                | 0:100                                  | --  |
| 2     | <b>5b</b>                | 0:100                                  | --  |
| 3     | <b>5a</b>                | 75:25                                  | 96:4  |
| 4     | <b>5b</b>                | 75:25                                  | 91:9  |
| 5     | <b>5a</b>                | 50:50                                  | 88:12   |
| 6     | <b>5b</b>                | 50:50                                  | 81:19   |
| 7     | <b>5a</b>                | 20:80                                  | 80:20   |
| 8     | <b>5b</b>                | 20:80                                  | 80:20   |
| 9     | <b>5a</b> <sup>[b]</sup> | 0:100                                  | 0:100   |

[a] Determined by HPLC after cargo delivery. [b] **UMUMOF-5a** recovered from a C<sub>60</sub> loading and releasing experiment.

saturated solution of pure C<sub>70</sub> (Table 1, entry 9). We determined a loading of 3.2 wt% of C<sub>70</sub> inside the such reused MOF **5a**, which seems to confirm this hypothesis. Delightfully, the sequential purification of a solution of C<sub>60</sub>:C<sub>70</sub> (40:60) by using the UMUMOF **5a** provided a pure C<sub>70</sub> solution after three cycles of uptake and release (see section 14.2 in the Supporting Information).

Aiming to visualize the incorporation of C<sub>60</sub> into MOFs **5a,b** we computed the simplified models C<sub>60</sub>@[Cu<sub>2</sub>O<sub>4</sub>-4]<sub>2</sub> and C<sub>60</sub>@[Zn<sub>2</sub>O<sub>4</sub>-4]<sub>2</sub> by using the GFN2-xtb method, recently developed by S. Grimme and coworkers.<sup>46</sup> These theoretical models consider two macrocycles connected to two dinuclear metal dimers and a C<sub>60</sub> unit placed in the concave curved pocket between both macrocyclic linkers. These calculations predict that the presence of the fullerene induces a structural distortion in the crystalline array. The four *p*-xylylene rings of both macrocycles adopt a twisted disposition in order to maximize the π-π stacking interactions with the fullerene. Furthermore, the angle between both macrocycles increases in relation to that measured in **5a,b** (C<sub>60</sub>@[Cu<sub>2</sub>O<sub>4</sub>-4]<sub>2</sub> = 96.3°; C<sub>60</sub>@[Zn<sub>2</sub>O<sub>4</sub>-4]<sub>2</sub> = 97.5°) whereas the distance between the two clusters is around 3 Å shorter. As a result, the distance between the centroids of the *p*-xylylene rings of each macrocycle slightly increases when compared with that distance in the pristine materials, thus assisting the effective encapsulation of fullerene derivatives by these metallopolymers (Figures 1a and 3).

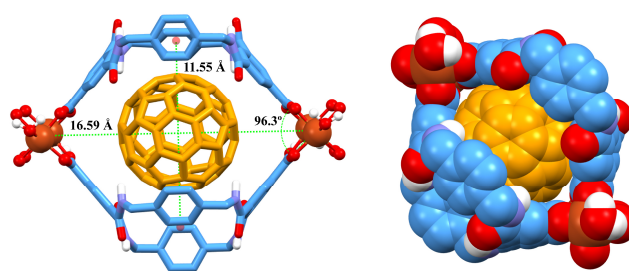


**Figure 3.** Computed model of C<sub>60</sub>@[Cu<sub>2</sub>O<sub>4</sub>-4]<sub>2</sub> (nonpolar hydrogen atoms have been omitted for clarity).

In summary, we have shown that structurally stable periodic 1D metal-organic frameworks can be prepared by coordination of copper(II) or zinc(II) clusters with a flexible benzylic amide macrocyclic diacid as a linker. These polymers were fully characterized by a range of spectroscopic and analytical techniques, including their structure elucidation by single-crystal X-ray diffraction. We successfully performed host-guest experiments in the solid state based on the fact that the concave pockets generated between two boat-like macrocycles show a size slightly larger than the van der Waals radii of the fullerene C<sub>60</sub>. Computational studies were also carried out, confirming that the establishment of π-π stacking interactions between the aromatic rings of the *p*-xylylenediamine moieties of the macrocycles and the fullerene surface stabilized its inclusion into the polymeric network. These polymers can absorb up to an impressive 34 wt% of C<sub>60</sub> guest molecules. We employed two methods for the releasing of the encapsulated guest, one that partially collapsed the framework and another that allowed the material to be reused. These systems are shown to be notably selective for the uptaking of C<sub>60</sub> from mixtures with the larger C<sub>70</sub> fullerene. We foresee that the concave pocket generated between benzylic amide macrocycles in these MOFs could play an important role in the encapsulation of other large molecules that could interact with the cavity through aromatic-aromatic or hydrogen bonding interactions.

## Acknowledgements

This research was supported by the MINECO and MICINN (CTQ2017-87231-P, PID2020-113686GB-I00 and RYC-2017-22700) and Fundación Séneca-CARM (Project 20811/PI/18). A. S.-S. thanks to the Fundación Séneca-CARM for his Ph.D. fellowship (20259/FPI/17). The authors also thank the computer resources at Cibeles and the technical support provided by the Centro de Computación Científica-UAM (RES-QSB-2019-3-0012).

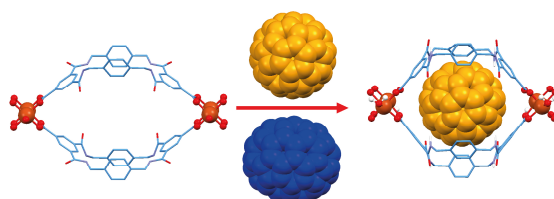
**Keywords:** metal-organic frameworks (MOFs) • macrocycles • C<sub>60</sub> fullerene • molecular recognition • host-guest systems

- [1] a) M. E. Davis, *Nature* **2002**, *417*, 813–821; b) Leonard R. MacGillivray (ed.) in *Metal-Organic Frameworks: Design and Application*, Wiley-VCH, **2010**; b) F. Tang, L. Li, D. Chen, *Adv. Mater.* **2012**, *24*, 1504–1534; c) K. Li, J. Garcia Martinez, (ed.) *Mesoporous Zeolites: Preparation, Characterization and Applications*. WILEY-VCH (**2014**)

- [2] a) O. M. Yaghi, M. O'Keeffe, N. W. Ockwig, H. K. Chae, M. Eddaoudi, J. Kim, *Nature* **2003**, *423*, 705–714; b) O. M. Yaghi, M. J. Kalmutzki, C. S. Diercks *Introduction to Reticular Chemistry Metal-Organic Frameworks and Covalent Organic Frameworks*, Wiley-VCH, **2019**.
- [3] a) O. M. Yaghi, H. Li, *J. Am. Chem. Soc.* **1995**, *117*, 10401–10402; b) S. L. James, *Chem. Soc. Rev.* **2003**, *32*, 276–288.
- [4] H. Deng, C. J. Doonan, H. Furukawa, R. B. Ferreira, J. Towne, C. B. Knobler, B. Wang, O. M. Yaghi, *Science* **2010**, *327*, 846–850.
- [5] a) H.-C. Zhou, J. R. Long, O. M. Yaghi, *Chem. Rev.* **2012**, *112*, 673–1268; b) H. Furukawa, K. E. Cordova, M. O'Keeffe, O. M. Yaghi, *Science* **2013**, *341*, 1230444.
- [6] a) H. Li, M. Eddaoudi, M. O'Keeffe, O. M. Yaghi, *Nature* **1999**, *402*, 276–279; b) M. Eddaoudi, D. B. Moler, H. Li, B. Chen, T. M. Reineke, M. O'Keeffe, O. M. Yaghi, *Acc. Chem. Res.* **2001**, *34*, 319–330; c) D. J. Tranchemontagne, J. L. Mendoza-Cortés, M. O'Keeffe, O. M. Yaghi, *Chem. Soc. Rev.* **2009**, *38*, 1257–1283; d) J. J. Perry, J. A. Perman, M. J. Zaworotko, *Chem. Soc. Rev.* **2009**, *38*, 1400–1417; e) S. Yuan, L. Feng, K. Wang, J. Pang, M. Bosch, C. Lollar, Y. Sun, J. Qin, X. Yang, P. Zhang, Q. Wang, L. Zou, Y. Zhang, L. Zhang, Y. Fang, J. Li, H.-C. Zhou, *Adv. Mater.* **2018**, *30*, 1704303.
- [7] Z.-J. Lin, J. Lü, M. Hong, R. Cao, *Chem. Soc. Rev.* **2014**, *43*, 5867–5895.
- [8] H. Zhang, R. Zou, Y. Zhao, *Coord. Chem. Rev.* **2015**, *292*, 74–90.
- [9] a) Q. W. Li, W. Y. Zhang, O. S. Miljanić, C. H. Sue, Y. L. Zhao, L. H. Liu, C. B. Knobler, J. F. Stoddart, O. M. Yaghi, *Science* **2009**, *325*, 855–859; b) C. Valente, E. Choi, M. E. Belowich, C. J. Doonan, Q. Li, T. B. Gasa, Y. Y. Botros, O. M. Yaghi, J. F. Stoddart, *Chem. Commun.* **2010**, *46*, 4911–4913; c) D.-W. Lim, S. A. Chyun, M. P. Suh, *Angew. Chem. Int. Ed.* **2014**, *53*, 7819–7822; *Angew. Chem.* **2014**, *126*, 7953–7956.
- [10] T.-H. Chen, I. Popov, Y.-C. Chuang, Y.-S. Chen, O. Š. Miljanić, *Chem. Commun.* **2015**, *51*, 6340–6342.
- [11] W.-Y. Gao, Y. Niu, Y. Chen, L. Wojtas, J. Cai, Y.-S. Chen, S. Ma, *CrystEngComm* **2012**, *14*, 6115–6117.
- [12] a) R. A. Smaldone, R. S. Forgan, H. Furukawa, J. J. Gassensmith, A. M. Slawin, O. M. Yaghi, J. F. Stoddart, *Angew. Chem. Int. Ed.* **2010**, *49*, 8630–8634; *Angew. Chem.* **2010**, *122*, 8812–8816; b) J. J. Gassensmith, H. Furukawa, R. A. Smaldone, R. S. Forgan, Y. Y. Botros, O. M. Yaghi, J. F. Stoddart, *J. Am. Chem. Soc.* **2011**, *133*, 15312–15315; c) R. S. Forgan, R. A. Smaldone, J. J. Gassensmith, H. Furukawa, D. B. Cordes, Q. Li, C. E. Wilmer, Y. Y. Botros, R. Q. Snurr, A. M. Slawin, J. F. Stoddart, *J. Am. Chem. Soc.* **2012**, *134*, 406–417.
- [13] a) S. J. Dalgarno, J. L. Atwood, C. L. Raston, *Cryst. Growth Des.* **2007**, *7*, 1762–1770; b) W. Liao, C. Liu, X. Wang, G. Zhu, X. Zhao, H. Zhang, *CrystEngComm* **2009**, *11*, 2282–2284; c) Y.-J. Liu, J.-S. Huang, S. S.-Y. Chui, C.-H. Li, J.-L. Zuo, N. Zhu, C.-M. Che, *Inorg. Chem.* **2008**, *47*, 11514–11518.
- [14] X. Feng, K. Chen, Y.-Q. Zhang, S.-F. Xue, Q.-J. Zhu, Z. Tao, A. I. Day, *CrystEngComm* **2011**, *13*, 5049–5051.
- [15] a) N. L. Strutt, D. Fairen-Jimenez, J. Iehl, M. B. Lalonde, R. Q. Snurr, O. K. Farha, J. T. Hupp, J. F. Stoddart, *J. Am. Chem. Soc.* **2012**, *134*, 17436–17439; b) N. L. Strutt, H. Zhang, J. F. Stoddart, *Chem. Commun.* **2014**, *50*, 7455–7458.
- [16] a) D. J. Cram, J. M. Cram, *Science* **1974**, *183*, 803–809; b) D. J. Cram, *Angew. Chem. Int. Ed. Engl.* **1988**, *27*, 1009–1020; c) D. J. Cram, J. M. Cram, *Container Molecules and Their Guests*; Royal Society of Chemistry: Cambridge, UK, **1994**.
- [17] a) R. B. Getman, Y.-S. Bae, C. E. Wilmer, R. Q. Snurr, *Chem. Rev.* **2012**, *112*, 703–723; b) K. Sumida, D. L. Rogov, J. A. Mason, T. M. McDonald, E. D. Bloch, Z. R. Herm, T.-H. Bae, J. R. Long, *Chem. Rev.* **2012**, *112*, 724–781; c) H. Wu, Q. Gong, D. H. Olson, J. Li, *Chem. Rev.* **2012**, *112*, 836–868; d) H. García and S. Navalón (ed.) in *Metal-Organic Frameworks: Applications in Separations and Catalysis*, Wiley-VCH, **2018**.
- [18] a) E. M. Pérez, N. Martín, *Chem. Soc. Rev.* **2008**, *37*, 1512–1519; b) C. Fuentes-Espinosa, M. Pujals, X. Ribas, *Chem* **2020**, *6*, 3219–3262; c) C. García-Simon, M. Costas, X. Ribas, *Chem. Soc. Rev.* **2016**, *45*, 40–62.
- [19] a) K. Tashiro, T. Aida, J.-Y. Zheng, K. Kinbara, K. Saigo, S. Sakamoto, K. Yamaguchi, *J. Am. Chem. Soc.* **1999**, *121*, 9477–9478; b) M.-Y. Ku, S.-J. Huang, S.-L. Huang, Y.-H. Liu, C.-C. Lai, S.-M. Peng, S.-H. Chiu, *Chem. Commun.* **2014**, *50*, 11709–11712; c) C. García-Simón, M. García-Borrás, Laura Gómez, T. Parella, Sílvia Osuna, J. Juanhuix, I. Imaz, D. MasPOCH, M. Costas, X. Ribas, *Nat. Commun.* **2014**, *5*, 5557; d) N. Kishi, M. Akita, M. Yoshizawa, *Angew. Chem. Int. Ed.* **2014**, *53*, 3604–3607; *Angew. Chem.* **2014**, *126*, 3678–3681; e) Y. Shi, K. Cai, H. Xiao, Z. Liu, J. Zhou, D. Shen, Y. Qiu, Q.-H. Guo, C. Stern, M. R. Wasielewski, F. Diederich, W. A. Goddard III, J. F. Stoddart, *J. Am. Chem. Soc.* **2018**, *140*, 13835–13842; f) W.-K. Han, H.-X. Zhang, Y. Wang, W. Liu, X. Yan, T. Lia, Z.-G. Gu, *Chem. Commun.* **2018**, *54*, 12646–12649; g) W. Sun, Y. Wang, L. Ma, L. Zheng, W. Fang, X. Chen, H. Jiang, *J. Org. Chem.* **2018**, *83*, 14667–14675; h) T. A. Barendt, W. K. Myers, S. P. Cornes, M. A. Lebedeva, K. Porfyrakis, I. Marques, V. Félix, P. D. Beer, *J. Am. Chem. Soc.* **2020**, *142*, 349–364; i) S. Matsuzaki, T. Arai, K. Ikemoto, Y. Inokuma, M. Fujita, *J. Am. Chem. Soc.* **2014**, *136*, 17899–17901; j) E. C. Escudero-Adan, A. Bauza, L. P. Hernandez-Eguia, F. Wurthner, P. Ballester, A. Frontera, *CrystEngComm* **2017**, *19*, 4911–4919; k) C. García-Simon, C. Colombari, Y. A. Cetin, A. Gimeno, M. Pujals, E. Ubasart, C. Fuertes-Espinosa, K. Asad, N. Chronakis, M. Costas, J. Jimenez-Barbero, F. Feixas, X. Ribas, *J. Am. Chem. Soc.* **2020**, *142*, 16051–16063; l) X. Chang, S. Lin, G. Wang, C. Shang, Z. Wang, K. Liu, Y. Fang, P. J. Stang, *J. Am. Chem. Soc.* **2020**, *142*, 15950–15960.
- [20] a) G. Bastien, P. I. Dron, M. Vincent, D. Canevet, M. Allain, S. Goeb, M. Sallé, *Org. Lett.* **2016**, *18*, 5856–5859; b) D.-C. Yang, M. Li, C.-F. Chen, *Chem. Commun.* **2017**, *53*, 9336–9339; c) V. García-Calvo, J. V. Cuevas, H. Barbero, S. Ferrero, C. M. Álvarez, J. A. González, B. Díaz de Greñu, J. García-Calvo, T. Torroba, *Org. Lett.* **2019**, *21*, 5803–5807; d) G. Zango, M. Krug, S. Krishna, V. Mariñas, T. Clark, M. V. Martínez-Díaz, D. M. Guldí, T. Torres, *Chem. Sci.* **2020**, *11*, 3448–3459.
- [21] a) X. Lu, T. Y. Gopalakrishna, Y. Han, Y. Ni, Y. Zou, J. Wu, *J. Am. Chem. Soc.* **2019**, *141*, 5934–5941; b) J. Calbo, A. de Juan, J. Aragó, J. Villalva, N. Martín, E. M. Pérez, E. Ortí, *Phys. Chem. Chem. Phys.* **2019**, *21*, 11670–11675; c) V. G. Jiménez, A. H. G. David, J. M. Cuerva, V. Blanco, A. G. Campaña, *Angew. Chem. Int. Ed.* **2020**, *59*, 15124–15128; *Angew. Chem.* **2020**, *132*, 15236–15240; d) Y. Xu, B. Wang, R. Kaur, M. B. Minameyer, M. Bothe, T. Drewello, D. M. Guldí, M. von Delius, *Angew. Chem. Int. Ed.* **2018**, *57*, 11549–11553; *Angew. Chem.* **2018**, *130*, 11723–11727; e) Y. Xu, S. Gsanger, M. B. Minameyer, I. Imaz, D. MasPOCH, O. Shyshov, F. Schwer, X. Ribas, T. Drewello, B. Meyer, M. von Delius, *J. Am. Chem. Soc.* **2019**, *141*, 18500–18507; f) M. B. Minameyer, Y. Xu, S. Fruhwald, A. Gorling, M. von Delius, T. Drewello, *Chem. Eur. J.* **2020**, *26*, 8729–8741.
- [22] T. Kawauchi, A. Kitaura, M. Kawauchi, T. Takeichi, J. Kumaki, H. Iida, E. Yashima, *J. Am. Chem. Soc.* **2010**, *132*, 12191–12193.
- [23] a) H. K. Chae, D. Y. Siberio-Perez, J. Kim, Y. Go, M. Eddaoudi, A. J. Matzger, M. O'Keeffe, O. M. Yaghi, *Nature* **2004**, *427*, 523–527; b) Y. Inokuma, T. Arai, M. Fujita, *Nat. Chem.* **2010**, *2*, 780–783; c) C.-X. Yang, X.-P. Yan, *J. Mater. Chem.* **2012**, *22*, 17833–17841; d) M. E. Foster, J. D. Azoulay, B. M. Wong, M. D. Allendorf, *Chem. Sci.* **2014**, *5*, 2081–2090; e) Y. Feng, T. Wang, Y. Li, J. Li, J. Wu, B. Wu, L. Jiang, C. Wang, *J. Am. Chem. Soc.* **2015**, *137*, 15055–15060; f) M. Souto, J. Calbo, S. Mañas-Valero, A. Walsh, G. Minguez Espallargas, *Beilstein J. Nanotechnol.* **2019**, *10*, 1883–1893; g) V. Martínez, B. Karadeniz, N. Biliškov, I. Lončarić, S. Muratović, D. Žilić, S. M. Avdoshenko, M. Roslova, A. A. Popov, K. Užarević, *Chem. Mater.* **2020**, *32*, 10628–10640.
- [24] A. Saura-Sanmartín, A. Martínez-Cuevas, D. Bautista, M. R. B. Marzari, M. A. P. Martins, M. Alajarin, J. Berná, *J. Am. Chem. Soc.* **2020**, *142*, 13442–13449.
- [25] a) A. G. Johnston, D. A. Leigh, R. J. Pritchard, M. D. Deegan, *Angew. Chem. Int. Ed. Engl.* **1995**, *34*, 1209–1212; b) A. G. Johnston, D. A. Leigh, L. Nezhad, J. P. Smart, M. D. Deegan, *Angew. Chem. Int. Ed. Engl.* **1995**, *34*, 1212–1216; c) A. G. Johnston, D. A. Leigh, A. Murphy, J. P. Smart, M. D. Deegan, *J. Am. Chem. Soc.* **1996**, *118*, 10662–10663.
- [26] a) J. Berna, G. Bottari, D. A. Leigh, E. Perez, *Pure App. Chem.* **2007**, *79*, 39–54; b) M. R. Panman, B. H. Bakker, D. den Uyl, E. R. Kay, D. A. Leigh, W. J. Buma, A. M. Brouwer, J. A. J. Geenevasen, S. Woutersen, *Nat. Chem.* **2013**, *5*, 929–934; c) J. Berna, M. Alajarin, J. S. Martínez-Espín, L. Buriol, M. A. P. Martins, R.-A. Orenes, *Chem. Commun.* **2012**, *48*, 5677–5679.

- [27] Thread **1** was previously employed for the efficient synthesis of stable amide-based pseudorotaxanes: a) A. Saura-Sanmartin, A. Martinez-Cuezva, A. Pastor, D. Bautista, J. Berna, *Org. Biomol. Chem.* **2018**, *16*, 6980–6987; b) C. Lopez-Leonardo, A. Martinez-Cuezva, D. Bautista, M. Alajarin, J. Berna, *Chem. Commun.* **2019**, *55*, 6787–6790; c) A. Martinez-Cuezva, F. Morales, G. R. Marley, A. Lopez-Lopez, J.-C. Martinez-Costa, D. Bautista, M. Alajarin, J. Berna, *Eur. J. Org. Chem.* **2019**, 3480–3488.
- [28] a) A. Martinez-Cuezva, L. V. Rodrigues, C. Navarro, F. Carro-Guillen, L. Buriol, C. P. Frizzo, M. A. P. Martins, M. Alajarin, J. Berna, *J. Org. Chem.* **2015**, *80*, 10049–10059; b) A. Martinez-Cuezva, C. Lopez-Leonardo, D. Bautista, M. Alajarin, J. Berna, *J. Am. Chem. Soc.* **2016**, *138*, 8726–8729; c) A. Martinez-Cuezva, D. Bautista, M. Alajarin, J. Berna, *Angew. Chem. Int. Ed.* **2018**, *57*, 6563–6567; *Angew. Chem.* **2018**, *130*, 6673–6677.
- [29] Macrocycle **3** was previously synthesized by following a similar dethreading protocol from a tetrabutylsuccinamide-based pseudorotaxane, which was obtained in a poor 17% yield. Herein rotaxane **2**, with a tetrabutylfumaramide thread **1**, was isolated in a 34% yield, notably improving the previously reported protocol.
- [30] V. N. Vukotic, C. A. O'Keefe, K. Zhu, K. J. Harris, C. To, R. W. Schurko, S. J. Loeb, *J. Am. Chem. Soc.* **2015**, *137*, 9643–9651.
- [31] Deposition numbers 2062294 (for UMUMOF **5a**) and 2062295 (for UMUMOF **5b**) contain the supplementary crystallographic data for this paper. These data are provided free of charge by the joint Cambridge Crystallographic Data Centre and Fachinformationszentrum Karlsruhe Access Structures service [www.ccdc.cam.ac.uk/structures](http://www.ccdc.cam.ac.uk/structures).
- [32] a) H. Furukawa, J. Kim, N. W. Ockwig, M. O'Keefe, O. M. Yaghi, *J. Am. Chem. Soc.* **2008**, *130*, 11650–11661; b) A. Schoedel, M. Li, D. Li, M. O'Keefe, O. M. Yaghi, *Chem. Rev.* **2016**, *116*, 12466–12535.
- [33] B. H. Wilson, S. J. Loeb, *Chem* **2020**, *6*, 1604–1612.
- [34] The solvent-accessible voids of the networks were calculated with the PLATON SQUEEZE program: P. Vandersluis, A. L. Spek, *Acta Crystallogr. A* **1990**, *46*, 194–201.
- [35] In the case of **5b**, the calculation of the solvent-accessible volume of the framework revealed a comparable value of 48% of the total volume.
- [36] L. J. Bellamy, *The Infrared Spectra of Complex Molecules*, 3rd edition, Chapman Hall, London, **1980**, ch. 22, pp. 283–327.
- [37] a) N. Fu, J. M. Baumes, E. Arunkumar, B. C. Noll, B. D. Smith, *J. Org. Chem.* **2009**, *74*, 6462–6468; b) J. J. Gassensmith, J. M. Baumes, B. D. Smith, *Chem. Commun.* **2009**, 6329–6338; c) H. Fu, X. Shao, C. Chipot, W. Cai, *Chem. Sci.* **2017**, *8*, 5087–5094; d) A. Altieri, V. Aucagne, R. Carrillo, G. J. Clarkson, D. M. D'Souza, J. A. Dunnett, K. M. Mullen, *Chem. Sci.* **2011**, *2*, 1922–1928.
- [38] T. Tomiyama, S. Uchiyama, H. Shinahara, *Chem. Phys. Lett.* **1997**, *264*, 143–148.
- [39] Some examples on the interaction between benzylic amide macrocycles and C<sub>60</sub> fullerene in interlocked species: a) T. Da Ros, D. M. Guldi, A. F. Morales, D. A. Leigh, M. Prato, R. Turco, *Org. Lett.* **2003**, *5*, 689–691; b) A. Mateo-Alonso, G. Fioravanti, M. Marcaccio, F. Paolucci, D. C. Jagesar, A. M. Brouwer, M. Prato, *Org. Lett.* **2006**, *8*, 5173–5176; c) A. Mateo-Alonso, C. Ehli, G. M. A. Rahman, D. M. Guldi, G. Fioravanti, M. Marcaccio, F. Paolucci, M. Prato, *Angew. Chem. Int. Ed.* **2007**, *46*, 3521–3525; *Angew. Chem.* **2007**, *119*, 3591–3595; d) M. Barrejon, A. Mateo-Alonso, M. Prato, *Eur. J. Org. Chem.* **2019**, 3371–3383. For other fullerene-based rotaxanes see: e) Y. Xu, B. Wang, R. Kaur, M. B. Minameyer, M. Bothe, T. Drewello, D. M. Guldi, M. von Delius, *Angew. Chem. Int. Ed.* **2018**, *57*, 11549–11553; *Angew. Chem.* **2018**, *130*, 11723–11727; f) Y. Xu, R. Kaur, B. Wang, M. B. Minameyer, S. Gsaenger, B. Meyer, T. Drewello, D. M. Guldi, M. von Delius, *J. Am. Chem. Soc.* **2018**, *140*, 13413–13420.
- [40] This aromatic solvent is known to provide excellent solubilization of fullerenes. See: R. S. Ruoff, D. S. Tse, R. Malhotra, D. C. Lorents, *J. Phys. Chem.* **1993**, *97*, 3379–3383.
- [41] The latter washing portion was further analysed by HPLC and no C<sub>60</sub> peak was observed in the chromatogram.
- [42] Note that the original Leigh's benzylic amide macrocycle was ideally designed as a receptor for CO<sub>2</sub>. See references 25a,b.
- [43] C. Serre, F. Millange, C. Thouvenot, M. Nogues, G. Marsolier, D. Louër, G. Férey, *J. Am. Chem. Soc.* **2002**, *124*, 13519–13526.
- [44] Powder X-Ray diffraction pattern of **5a** after C<sub>60</sub> release revealing that material is still crystalline displaying most of the diffraction peaks at same theta values except an intense one which is shifted to higher angle values as a result of the macrocycle breathing (Figure S29).
- [45] a) R. S. Ruoff, D. S. Tse, R. Malhotra, D. C. Lorents, *J. Phys. Chem. Physics-Usp.* **1998**, *41*, 1091–1114.
- [46] C. Bannwarth, S. Ehlert, S. Grimme, *J. Chem. Theory Comput.* **2019**, *15*, 1652–1671.

## Entry for the Table of Contents



A ditopic flexible benzylic amide macrocycle was employed as organic ligand for the assembly of metal-organic frameworks. These reticular materials form non-interpenetrated channels with a remarkable 46% of solvent-accessible volume. The incorporation of fullerene  $C_{60}$  inside their adjustable pockets was studied, being able to occupy an impressive 98% of them. These materials were selective for the recognition of  $C_{60}$  in the presence of the larger  $C_{70}$ .

Institute and/or researcher Twitter usernames: @socumu\_lab